

Diurnal dynamics of the Arabidopsis rosette proteome and phosphoproteome

R. Glen Uhrig¹, Sira Echevarría-Zomeño¹, Pascal Schlapfer¹, Jonas Grossmann², Bernd Roschitzki², Niklas Koerber³, Fabio Fiorani³, and Wilhelm Gruissem⁴

¹ETH Zürich

²Functional Genomics Center Zurich

³Forschungszentrum Jülich GmbH

⁴ETH Zurich

October 12, 2020

Abstract

Plant growth depends on the diurnal regulation of cellular processes, but it is not well understood if and how transcriptional regulation controls diurnal fluctuations at the protein-level. Here we report a high-resolution Arabidopsis thaliana (Arabidopsis) leaf rosette proteome acquired over a 12 h light : 12 h dark diurnal cycle and the phosphoproteome immediately before and after the light-to-dark and dark-to-light transitions. We quantified nearly 5000 proteins and 800 phosphoproteins, of which 288 fluctuated in their abundance and 226 fluctuated in their phosphorylation status. Of the phosphoproteins, 60% were quantified for changes in protein abundance. This revealed six proteins involved in nitrogen and hormone metabolism that had concurrent changes in both protein abundance and phosphorylation status. The diurnal proteome and phosphoproteome changes involve proteins in key cellular processes, including protein translation, light perception, photosynthesis, metabolism and transport. The phosphoproteome at the light-dark transitions revealed the dynamics at phosphorylation sites in either anticipation of or response to a change in light regime. Phosphorylation site motif analyses implicate casein kinase II and calcium/calmodulin dependent kinases among the primary light-dark transition kinases. The comparative analysis of the diurnal proteome and diurnal and circadian transcriptome established how mRNA and protein accumulation intersect in leaves during the diurnal cycle of the plant.

Hosted file

PCE-20-0545_Uhrig et al 2020_manuscript_resubmission.pdf available at <https://authorea.com/users/325277/articles/486297-diurnal-dynamics-of-the-arabidopsis-rosette-proteome-and-phosphoproteome>

Figure 1

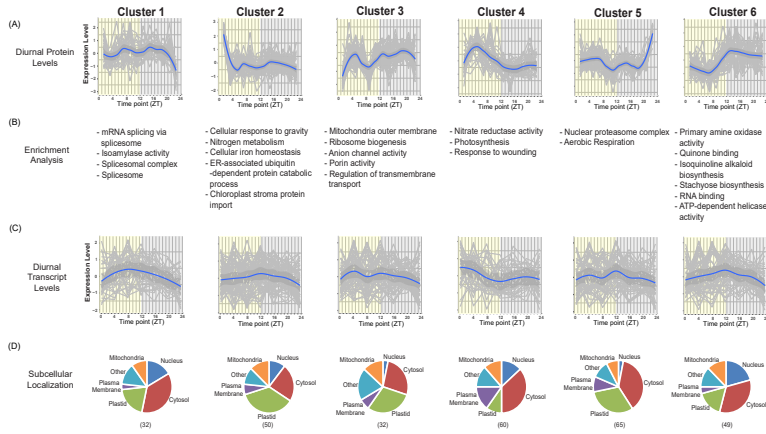


Figure 1: Analysis of the diurnal proteome: clustering, enrichment analysis and subcellular localization. (A) Significantly changing proteins (Fold-change (FC) ≥ 1.5 , ANOVA P value ≤ 0.05 , ≥ 2 peptides) were subjected to an unsupervised clustering analysis (GProX; <http://gprox.sourceforge.net>) resolving 6 protein clusters. Y- and X-axis depict standardized expression level and harvest time (Zeitgeber time, ZT), respectively. Median expression is depicted in blue. (B) Term enrichment analysis of significantly changing proteins using SelfRank (P value ≤ 0.01 , size ≥ 2). (C) Standardized diurnal transcript expression level of each corresponding clustered protein (Log10). Median expression is depicted in blue. Transcript expression level was obtained from Diurnal DB (<http://diurnal.moclerlab.org/>). (D) *In silico* subcellular localization analysis of significantly changing proteins using SUBAcon (SUBA3; <http://suba3.plant-energy.uwa.edu.au>). Bracketed numbers represent the number of proteins per cluster.

Figure 2

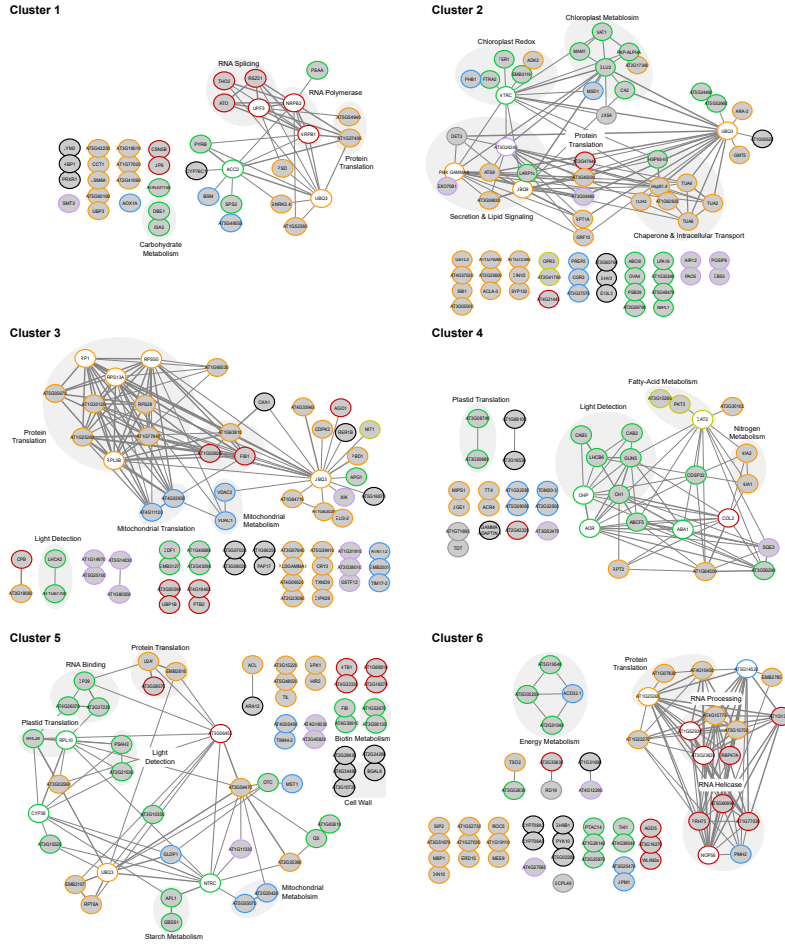


Figure 2: Interaction networks of the diurnal proteome. Using STRING-DB (<https://string-db.org/>), association network analysis of statistically significant diurnally changing proteins was performed using the generated unsupervised clusters (Figure 1). Edge thickness indicates confidence of the connection between two nodes (0.5 - 1.0). Changing proteins (grey circles) are labeled by either their primary gene annotation or Arabidopsis gene identifier (AGI). The colored outline of each node represents that proteins in silico predicted subcellular localization (SUBAcon; suba3.plantenergy.uwa.edu.au). Nucleus (red), cytosol (orange), plastid (green), mitochondria (blue), plasma membrane (purple), peroxisome (dark yellow), endoplasmic reticulum/golgi/secreted (black) are depicted. A second layer of STRING-DB identified proteins (white nodes) not found in each respective significantly changing protein cluster was used to highlight the interconnectedness of proteins in the cluster. Multiple nodes encompassed by a labeled grey circle represent proteins involved in the same cellular process.

Figure 3

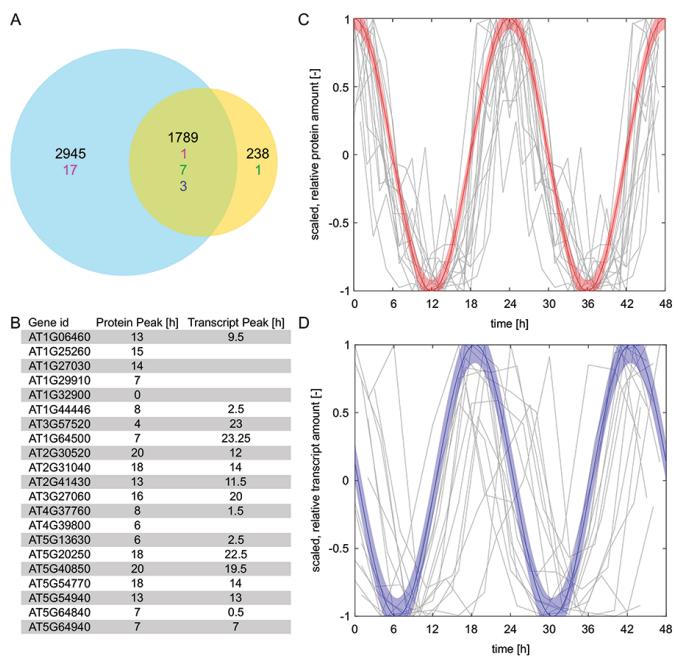
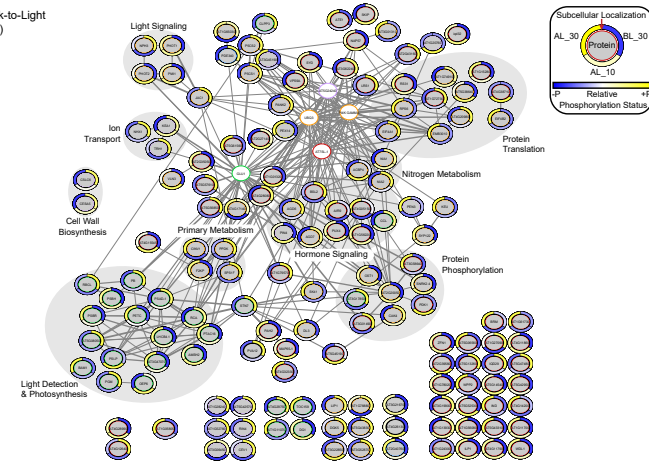


Figure 3: Comparative analysis of diurnal proteome to free-running circadian proteome (Krahmer et al., 2019). (A) Number of proteins measured in this study (blue circle) and Krahmer et al. (2019) (orange circle). Number of stable proteins (black), fluctuating proteins in our study only (magenta), Krahmer et al. (2019) only (green) and both studies (blue). (B) Table of 21 proteins that show significant (B, Q) fluctuation using JTK with their respective peak time period for protein and transcript levels (Diurnal DB, <http://diurnal.mocklerlab.org/>). (C and D) Normalized (Median = 0, Amplitude of 2) protein levels of 15 proteins both fluctuating in protein and transcript levels (gray lines) shifted to peak at time zero for protein levels in (C) and transcript levels in (D). Protein data was plotted twice to visualize a 48 h timeframe. The theoretical cosine functions with associated 99% confidence interval for protein levels (C, red) and transcript levels (D, blue) are shifted by 5.5 h.

Figure 4
(A) Dark-to-Light
(D-L)



(B) Light-to-Dark
(L-D)

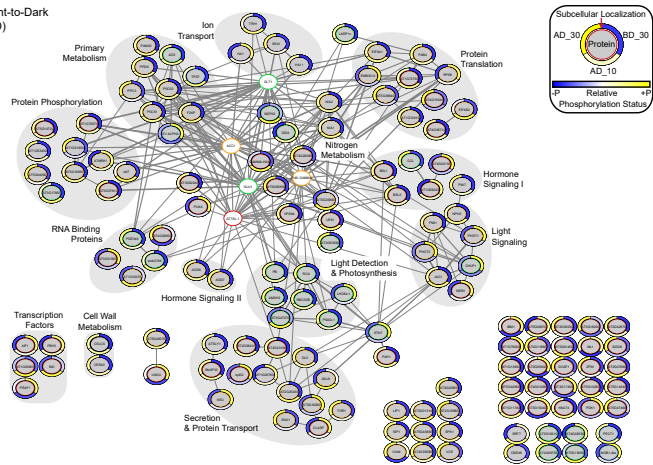


Figure 4: Interaction networks of the diurnal phosphoproteome at the D-L and L-D transitions. Using the STRING-DB, association network analysis of statistically significant diurnally changing phosphorylated proteins was performed (ANOVA P value ≤ 0.05). Edge thickness indicates strength of the connection between two nodes (0.5 - 1.0). Phosphorylated proteins (grey circles) are labeled by either their primary gene annotation or Arabidopsis gene identifier (AGI). Outer circle around each node depicts the standardized relative \log_2 FC in that proteins phosphorylation status between time-points. The sliding scale of yellow to blue represents a relative increase and decrease in phosphorylation, respectively. The inner colored circles represent *in silico* predicted subcellular localization (SUBAcon; suba3.plantenergy.uwa.edu.au). Nucleus (red), cytosol (orange), plastid (green), mitochondria (blue), plasma membrane (purple), peroxisome (dark yellow), endoplasmic reticulum/golgi/secreted (black) are depicted. A second shell of STRING-DB proteins (white circles) not found in our dataset was used to highlight the interconnectedness of the network. Multiple nodes encompassed by a labelled grey circle represent proteins involved in the same cellular process.

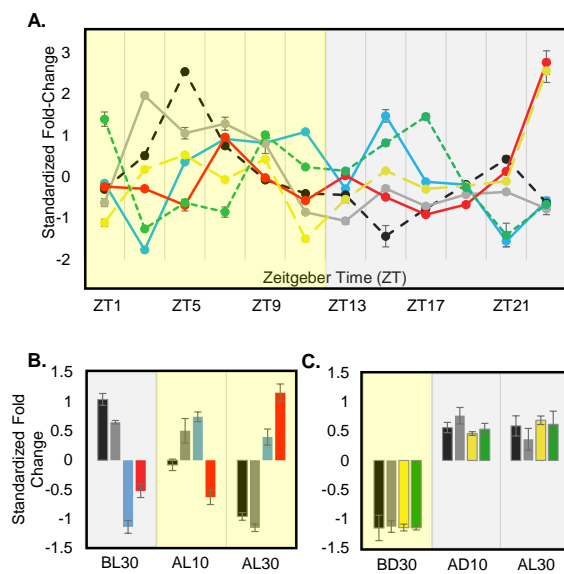


Figure 5: Proteins exhibiting a significant change in both diurnal protein abundance and protein phosphorylation status. Six proteins were found to significantly change in protein abundance and protein phosphorylation: AT1G10940 (SnRK2.4; blue), AT1G37130 (NIA2; black), AT1G77760 (NIA1; grey), AT4G32330 (TPX2; red), AT4G16340 (SPK1; yellow), AT4G35890 (LARP1c; green). (A) Diurnal protein abundance change profile. Standardized fold-change values are plotted relative to ZT. (B) D-L and (C) L-D phosphorylation change profiles. Standardized fold-change values are plotted relative to transition time-point either 10 or 30 minutes before light (BL), after light (AL), before dark (BD) or after dark (AD). Standard error bars are shown.

Figure 6

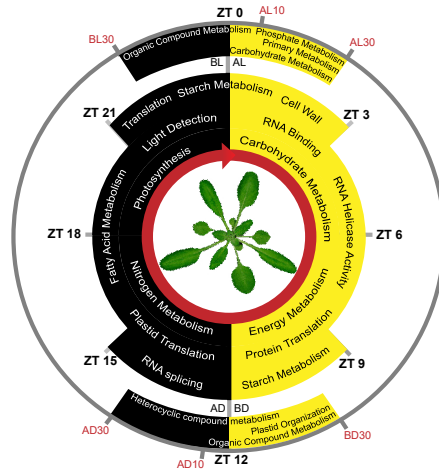


Figure 6: Schematic representation of Arabidopsis cellular and biological processes affected by diurnal fluctuations in protein abundance or protein phosphorylation. Inner terms represent processes maintaining proteins which exhibit a maximal change in abundance during the day (yellow) or night (black). Outer terms describe processes maintaining proteins undergoing changes in protein phosphorylation at the dark-to-light (D-L) transition (top) or light-to-dark (L-D) transition (bottom). The coverage of each inner ring relative to ZT0 (day) or ZT12 (night) represents the approximate time proteins (ZT) and phosphoproteins (30 min before light/dark and 10 or 30 min after light/dark) corresponding to each process exhibiting maximal change. The cellular and biological terms described here were obtained through GO term enrichment of each protein and phosphoprotein cluster as outlined in the materials and methods.

Table 1

Table 1: Proteome and Phosphoproteome coverage.

Identified, quantified and significantly changing diurnal proteins, phosphopeptides and phosphoproteins. Quantification confidence thresholds include: proteome: ≥ 2 proteotypic peptides; phosphoproteome: phosphorylation site probability ID ≥ 0.8 , quantified in ≥ 2 biological replicates and 3/3 transition time-points. Significance thresholds include: proteome: FC ≥ 1.5 and ANOVA P value ≤ 0.05 ; phosphoproteome: ANOVA P value ≤ 0.05 . Application of proteome and phosphoproteome significance thresholds are denoted by a single (*) and double (**) stars, respectively.

	Proteome	Phosphoproteome
Protein IDs	7060	1091
Peptide IDs	n/a	1776
Proteins Quantified	4762	725
Peptides Quantified	n/a	1056
Sig. Changing Proteins	*288	**226
Sig. Changing Peptides	n/a	**271

Table 2

Table 2: GSEA of significantly changing phosphoproteins at the D-L and L-D transition. GSEA was performed using SetRank (corr P value ≤ 0.01 ; FDR ≤ 0.05 , minProt = 2).

D-L Transition					
Name	Description	Database	Size	SetRank	Corr P value
GO:0016020	membrane	GOCC	273	0.125972	0.000913639
GO:0005524	ATP binding	GOMF	104	0.110291	0.006818059
GO:0009416	response to light stimulus	GOBP	32	0.059617	0.000197647
M00428	eIF4F complex	KEGG	4	0.032225	0.000207554
GO:0005618	cell wall	GOCC	20	0.059617	0.000666835
GO:0009941	chloroplast envelope	GOCC	33	0.032225	0.000828511
GO:0009785	blue light signaling pathway	GOBP	2	0.032225	0.001166915
GO:0016310	phosphorylation	GOBP	60	0.032225	0.001933236
GO:0046527	glucosyltransferase activity	GOMF	5	0.032225	0.007552696
GO:0015291	transmembrane transporter activity	GOMF	9	0.032225	0.008195815
GO:0048528	post-embryonic root development	GOBP	10	0.032225	0.004122321
META_PWY-101	photosynthesis light reactions	BIOCYC	3	0.032225	0.004299686
GO:0009523	photosystem II	GOCC	2	0.032225	0.004363247
GO:0009555	pollen development	GOBP	6	0.032225	0.005631461
GO:1902580	single-organism cellular localization	GOBP	12	0.032225	0.005682244
ath04141	Protein processing in endoplasmic reticulum	KEGG	5	0.032225	0.007587253
GO:0050832	defense response to fungus	GOBP	11	0.032225	0.007657975
GO:0042126	nitrate metabolic process	GOBP	5	0.032225	0.009137088
GO:0003924	GTPase activity	GOMF	6	0.032225	0.009196556
L-D Transition					
Name	Description	Database	Size	SetRank	Corr P value
GO:0009507	chloroplast	GOCC	116	0.130435	0.000316305
GO:0009108	coenzyme biosynthetic process	GOBP	3	0.048309	0.002527376
GO:0016903	oxidoreductase activity	GOMF	4	0.048309	0.005222496
GO:0005829	cytosol	GOCC	213	0.048309	0.007059263
GO:0016310	phosphorylation	GOBP	52	0.048309	0.009610197
GO:0006997	nucleus organization	GOBP	3	0.048309	0.000925019
GO:0009637	response to blue light	GOBP	9	0.048309	0.001227825
GO:0009573	RuBisCO complex	GOCC	2	0.048309	0.00637449
GO:0009785	blue light signaling pathway	GOBP	2	0.048309	0.006496782
GO:0010359	regulation of anion channel activity	GOBP	2	0.048309	0.006496782
GO:0009416	response to light stimulus	GOBP	31	0.048309	0.008163336
GO:0016192	vesicle-mediated transport	GOBP	31	0.048309	0.002856364
GO:0090407	organophosphate biosynthetic process	GOBP	11	0.048309	0.003001091
GO:0097306	cellular response to alcohol	GOBP	11	0.048309	0.004964197
GO:0003924	GTPase activity	GOMF	6	0.048309	0.006375452
GO:0071365	cellular response to auxin stimulus	GOBP	8	0.048309	0.008146711

Table 3

Table 3 : Proteins involved in plant cell processes with independent changes in abundance and/or phosphorylation.

Biological Process	AGI	Name	Description	Abundance (A) / Phosphorylation (P)
Translation	AT5G54940	eIF1	Translation initiation factor SU11 family protein	A
	AT1G72340	eIF2Bc-a	NagB/RpiA/CoA transferase-like superfamily protein	A
	AT1G27400	RPL17A	Ribosomal protein L22p/L17e family protein	A
	AT1G33120	RPL9B	Ribosomal protein L6 family	A
	AT4G10450	RPL9D	Ribosomal protein L6 family	A
	AT1G77940	RPL30B	Ribosomal protein L7Ae/L30e/S12e/Gadd45 family	A
	AT3G45030	RPS20A	Ribosomal protein S10p/S20e family protein	A
	AT5G64140	RPS28C	Ribosomal protein S28	A
	AT3G02560	RPS7B	Ribosomal protein S7e family protein	A
	AT1G25260		Ribosomal protein L10 family protein	A
	AT5G24490	mito30S	30S ribosomal protein	A
	AT1G07830	mitoL29	Ribosomal protein L29 family protein	A
	AT4G11120	mitoEF-Ts	Translation elongation factor Ts (EF-Ts)	A
	AT3G08740	chloroEF-P	Elongation factor P (EF-P) family protein	A
	AT5G54600	chloroL24	Translation protein SH3-like family protein	A
	AT1G13020	eIF4B	Eukaryotic initiation factor 4B2	P
	AT3G13920	eIF4A	Eukaryotic translation initiation factor 4A1	P
	AT5G38640	eIF2Bc-d	NagB/RpiA/CoA transferase-like superfamily protein	P
	AT3G13920	eIF4A	Eukaryotic translation initiation factor 4A1	P
	AT4G20980	eIF3-d	Eukaryotic translation initiation factor 3 subunit 7	P
AT4G31700	RPS6A	Ribosomal protein S6	P	
AT5G10360	RPS6B	Ribosomal protein S6e	P	
AT2G23350	PABP	Poly(A) binding protein 4	P	
Fatty Acid & Lipid Biosynthesis	AT2G33150	KAT2/PKT3	Peroxisomal 3-ketoacyl-CoA thiolase 3	A
	AT3G15290	MFP2/AIM1-like	3-hydroxyacyl-CoA dehydrogenase family protein	A
Primary Metabolism	AT1G77760	NIA1	Nitrate reductase 1	P
	AT1G37130	NIA2	Nitrate reductase 2	P
	AT2G42600	PEPC2	Phosphoenolpyruvate carboxylase 2	P
	AT3G14940	PEPC3	Phosphoenolpyruvate carboxylase 3	P
	AT5G20280	SPS1F	Sucrose phosphate synthase 1F	P
Carbohydrate Metabolism	AT1G32900	GBSS1	Granule bound starch synthase 1	A
	AT5G19220	ADG2	ADP glucose pyrophosphorylase	A
	AT1G03310	DBE1	Debranching enzyme 1	A
	AT3G23920	BAM1	Beta-amylase 1	P
Cell wall	AT5G09870	CESA5	Cellulose synthase 5	P
	AT3G07330	CSLC6	Cellulose-synthase-like C6	P
	AT2G18960	HA1	H ⁺ -ATPase 1	P